Nonlinear Permeability Measurements for Nickel Zinc Ferrite and Nickel Zinc Ferrite/Barium Strontium Titanate Composites From 1 to 4 GHz

Travis D. Crawford[1], Andrew J. Fairbanks[1], Julio A. Hernandez[2], Tyler N. Tallman[2], and Allen L. Garner[1,3,4]

[1]School of Nuclear Engineering, Purdue University, West Lafayette, IN 47906 USA
[2]School of Aeronautics and Astronautics, Purdue University, West Lafayette, IN 47907 USA
[3]School of Electrical and Computer Engineering, Purdue University, West Lafayette, IN 47907 USA
[4]Department of Agricultural and Biological Engineering, Purdue University, West Lafayette, IN 47907 USA

Nonlinear transmission lines (NLTLs), which exhibit permittivity as a function of electric field and/or permeability as a function of magnetic field strength, are of increasing importance for sharpening pulses to less than 100 ps and serving as radio frequency (RF) sources; however, NLTLs often are not easily modified to achieve different output parameters. One method under investigation involves combining nonlinear dielectric [barium strontium titanate (BST)] and/or magnetic [nickel zinc ferrite (NZF)] inclusions to tune the NLTL properties by adjusting the inclusion loading fractions. This article focuses on measuring the nonlinear permeability and magnetic loss tangent of composites comprising various volume loadings of NZF or NZF and BST inclusions encapsulated in a silicon matrix. We measured the relative permeability from 1 to 4 GHz using a coaxial airline while biasing the samples in an external dc magnetic field from 0 to 171 kA/m. The permeability decreased from 1 to 4 GHz for each volume fraction but increased with increasing magnetic field strength at low-magnetic field strengths with sufficient NZF volume loading. The magnetic loss tangent of the composites increased with increasing frequency and/or NZF volume fraction but was suppressed by increasing the external magnetic field strength. Adding BST to NZF composites did not cause a significant change in permeability compared to NZF alone, based on an analysis of variance (ANOVA) and multiple comparison test. These results elucidate the frequency dependence of NZF volume loading at microwave frequency and provide initial information for simulating NLTLs and examining more comprehensive RF system behavior.

Index Terms—**Barium strontium titanate (BST), high-power microwaves (HPMs), magnetic properties, nickel zinc ferrite (NZF), nonlinear transmission lines (NLTLs).**

I. Introduction

NONLINEAR transmission lines (NLTLs) offer a robust, solid-state solution for generating high-power microwaves (HPMs). Unlike conventional vacuum microwave sources, NLTLs employ nonlinear materials whose dielectric and/or magnetic properties vary with voltage and current, respectively, to modulate a delivered pulse [1]–[3]. Geometry and material selection can greatly impact NLTL performance, motivating material development and characterization at microwave frequencies. Nonlinear materials, such as barium strontium titanate (BST) and nickel zinc ferrite (NZF), are used in various NLTL topologies for their nonlinear permittivity and permeability, respectively [1], [3]. Both materials, albeit by different means, aid in generating an electromagnetic shockwave governed by the inverse relationship between phase velocity and the material's permeability and permittivity. In ferrite-based lines, often called gyromagnetic lines, the propagation of the shockwave results in the dampened gyromagnetic precession of the material's magnetic moments around the effective magnetic field [3]–[5]. Gyromagnetic NLTLs often bias nonlinear ferrimagnetic material in an external magnetic field to allow for coherent precession of the magnetic moments. This can increase the peak output power of the system and generate sharper risetimes [4].

Magnetization motion is governed by the Landau–Lifshitz–Gilbert (LLG) equation, given in SI units by [6]

$$\frac{\partial \mathbf{M}}{\partial t} = (-\gamma_0 \mathbf{M} \times \mathbf{H}_{\mathbf{eff}}) + \left(\alpha \mathbf{M} \times \frac{\partial \mathbf{M}}{\partial t}\right) \tag{1}$$

where $\mathbf{M}$ is the magnetization, $\mathbf{H}_{\mathbf{eff}}$ is the effective magnetic field, γ is the gyromagnetic factor (with units of $\mathrm{A}^{-1} \cdot \mathrm{s}^{-1} \cdot \mathrm{m}$), and α is the dimensionless damping constant for spin (typical values $0.01 < \alpha < 1$ [4]). In (1), the first term describes the precession of the magnetic moment about $\mathbf{H}_{\mathbf{eff}}$ and the second term describes the damping of the moment.

Unlike ferrites, it is hypothesized that BST generates microwaves by exploiting the titanate's crystalline structure [7]. When in a ferroelectric state, the titanate's structure permits the formation of a permanent dipole [3], [7], which is removed when the structure is brought to the Curie temperature and enters a paraelectric state [7]. The oscillations occur due to the motion of the polarization vector around the crystalline lattice.

Combinations of ferroelectric materials and ferrites have been explored for various applications. For example, ferrite

Manuscript received November 19, 2020; revised February 20, 2021; accepted March 20, 2021. Date of publication March 25, 2021; date of current version May 17, 2021. Corresponding author: A. L. Garner (e-mail: algarner@purdue.edu).

Color versions of one or more figures in this article are available at https://doi.org/10.1109/TMAG.2021.3068820.

Digital Object Identifier 10.1109/TMAG.2021.3068820

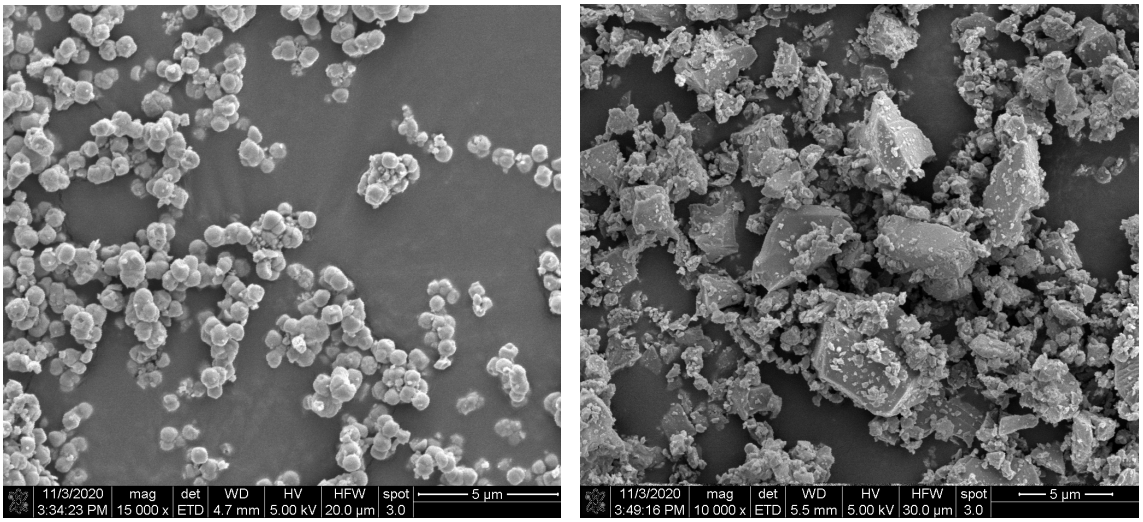

Fig. 1. SEM scans of BST (left) and NZF (right). The images show that the BST inclusions had a spherical geometry while the NZF inclusions typically had aspect ratios of less than unity.

cores in high-energy density capacitors were coated with barium titanate to increase the permittivity of the capacitors [1]. Other studies have shown that adjusting volume fraction, inclusion aspect ratio, and inclusion shapes facilitated the tuning of the material's electromagnetic properties [9], [11]. Similarly, manipulating the volume fractions of BST and NZF inclusions permit the adjustment of a composite's bulk permittivity and permeability [10]–[15].

Composites containing ferrites have been developed in numerous studies [16]–[22]. However, their nonlinear behavior is seldom measured and discussed in the context of application to NLTLs. Moreover, the combination of materials presented here has implications on the development of hybrid NLTLs that utilize both ferroelectric and ferrimagnetic bulk materials [3]. While characterizing the material's nonlinear behavior is paramount for NLTL systems, these prior studies have only considered material in the nonlinear regime at sub-gigahertz frequencies or the linear regime at microwave frequencies. Implementing these materials into HPM sub-systems, such as NLTLs, requires characterizing this nonlinear behavior at microwave frequencies.

This study evaluates the nonlinear permeability of single- and dual-inclusion coaxial composites between 1 and 4 GHz to better understand their electromagnetic behavior and potential application for flexible HPM and NLTL systems. Section II summarizes the experimental materials and methods. Section III reports the measurements of permeability as a function of magnetic field strength for composites containing NZF inclusions or a combination of NZF and BST inclusions. We make concluding remarks in Section IV.

II. Methods

We manufactured single-inclusion composites containing various volume fractions of NZF and dual-inclusion composites with various volume fractions of NZF and BST. Table I summarizes the volume fractions used in these composites.

TABLE I
Volume Fractions of NZF and BST Used in Single- and Dual-Inclusion Composites

Single Inclusion NZF (%)	Dual Inclusion (BST/NZF) (%)	
5	5	5
10	5	10
15	10	5
20	10	10
25	10	15
/	15	10

Four samples of each volume fraction were fabricated to quantify the statistical variations in permeability measurements and to evaluate the reproducibility of the manufacturing procedure.

All composites used a two-part silicone (Sylgard 184) as their host. The composites were manufactured with length $l \geq \lambda/4$, where λ is the wavelength, based on the lowest measured frequency with an inner diameter of 3 mm, and an outer diameter of 7 mm. SEM revealed that the NZF inclusions mostly had aspect ratios typically less than unity while the BST inclusions were generally spherical, as shown in Fig. 1. The manufacturers of the NZF (Powder Processing & Technology FP350) and BST (TPL, Inc. HBS-8000) powders reported average inclusion sizes of 17 μm and 600–800 nm, respectively, although SEM suggests a lower average inclusion size for the NZF inclusions. X-ray diffraction (XRD) performed on both the NZF and BST powders showed that the composition agreed well with the literature/commercial compositions of $Ni_{0.5}Zn_{0.5}Fe_2O_4$ and $Ba_{0.45}Sr_{0.55}TiO_3$ [15].

The NZF powder has a reported magnetization saturation of 150 kA/m and bulk density of approximately 2 g/cm^3. The curie temperature is reported as 350 °C and has a resistivity of 10^9 Ω/cm at 100 V. Due to the difficult geometry of this

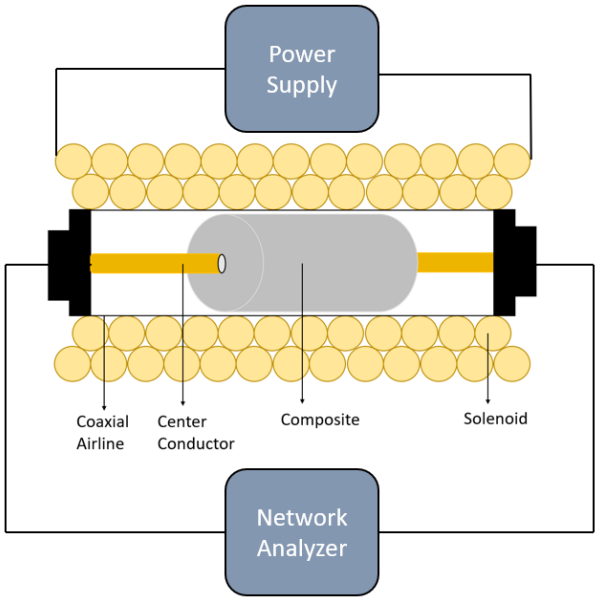

Fig. 2. Experimental setup for measuring the nonlinear permeability of the composites. The composite was placed on the center conductor of the coaxial airline, which was placed inside a solenoid. After energizing the solenoid, the S-parameters were then measured and imported them into commercial software to extract the permeability.

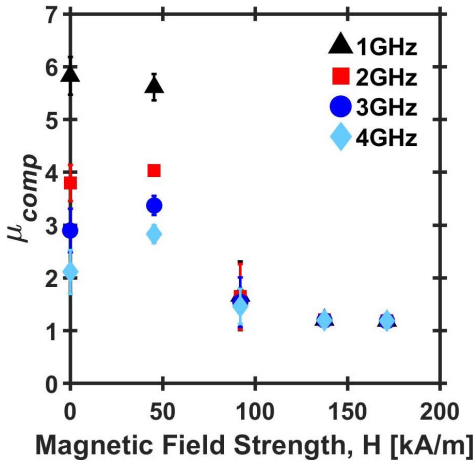

Fig. 3. Real component of the relative permeability μ_{comp} of a composite consisting of 50% NZF inclusions in PDMS as a function of bias magnetic field strength at 1, 2, 3, and 4 GHz. The 50% NZF was used to establish a baseline value for the permeability of the bulk ferrite. The values reported are the mean of four measurements with error bars determined using standard deviation.

setup, we have appealed to percolation theory for establishing a baseline bulk permeability of the NZF at our frequencies. A 50% NZF sample was manufactured and measured, which is well above the suggested 30% percolation threshold for spherical inclusions [23]–[25]. The permeability of this composite at 1 GHz with no applied magnetic field was approximately 5.8 at 30 °C (see Fig. 3), which is similar to the values reported elsewhere at 100 kHz [26], [27]. The BST powder has a reported density of 5.4 g/cm^3 and estimated bulk relative permittivity of 5990 at 30 °C at 100 kHz.

The composites were manufactured by first measuring the mass of the PDMS base and then calculating the mass of

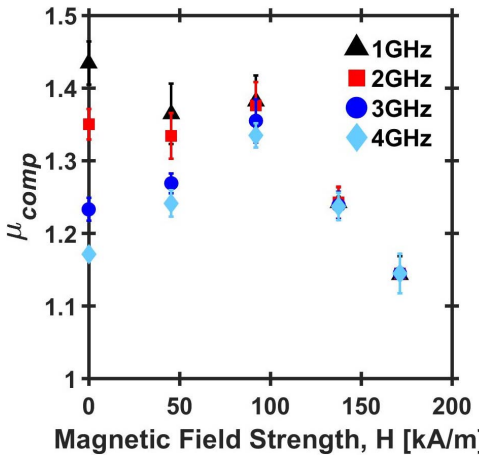

Fig. 4. Real component of the relative permeability μ_{comp} of a composite consisting of 25% NZF inclusions in PDMS as a function of bias magnetic field strength at 1, 2, 3, and 4 GHz. The values reported are the mean of four measurements with error bars determined using standard deviation.

the powder needed to reach a desired volume fraction. The mixture was then mixed using a planetary centrifuge (Thinky Mixer AR-100) at 400 r/min. Composites containing BST were bath sonicated (Crest Ultrasonics CP200HT) for 4 h to break up conglomerations. We added the necessary amount of curing agent, 1/10th the mass of PDMS, and stirred the mixture by hand for 5 min. Both single- and dual-inclusion composites were then outgassed (Medline Scientific Jeio Tech 665L Vacuum Oven OV-12) for 5 min at 0.1 MPa before placement into a mold. The molds were then outgassed for 5 min to ensure no air bubbles formed during the filling process. The samples were then placed into an oven (Blue M LO-136E) at 100 °C for 2 h to cure.

We next designed and constructed a multilayered dc solenoid. The solenoid frame was approximately 120 mm long; the solenoid was wrapped in 1200 turns of 14 Gauge magnet wire 1.71 mm in diameter (with insulation) using a coil winding machine. The inner diameter of the solenoid frame was 1 in to fit a coaxial airline (Keysight Type-N 50 Ω Verification Kit) inside. The coaxial airline had a length of 10.87 cm. The solenoid was wired to a current supply (Acopian Model #: Y050LX2B2880-DIO1) with a maximum output current of 28 A at 50 V. A digital interface communicated with the power supply by a computer to control the current and voltage ramp rate. Two fans were placed on each side of the coil to minimize the temperature increase, especially at higher currents. Internal temperatures were measured at three locations inside the solenoid frame using a digital infrared thermometer before and after each measurement to assess the uniformity and severity of the heating. A Gauss meter and axial probe (F.W. Bell 5186-110120) were used to measure the magnetic field to ensure field uniformity and strength inside the solenoid. Fig. 2 shows the experimental setup.

We accounted for losses associated with the coaxial airline by performing a full two-port calibration with the airline attached using a Keysight 85054D Calibration Kit. This calibration type achieves the most accurate measurement by

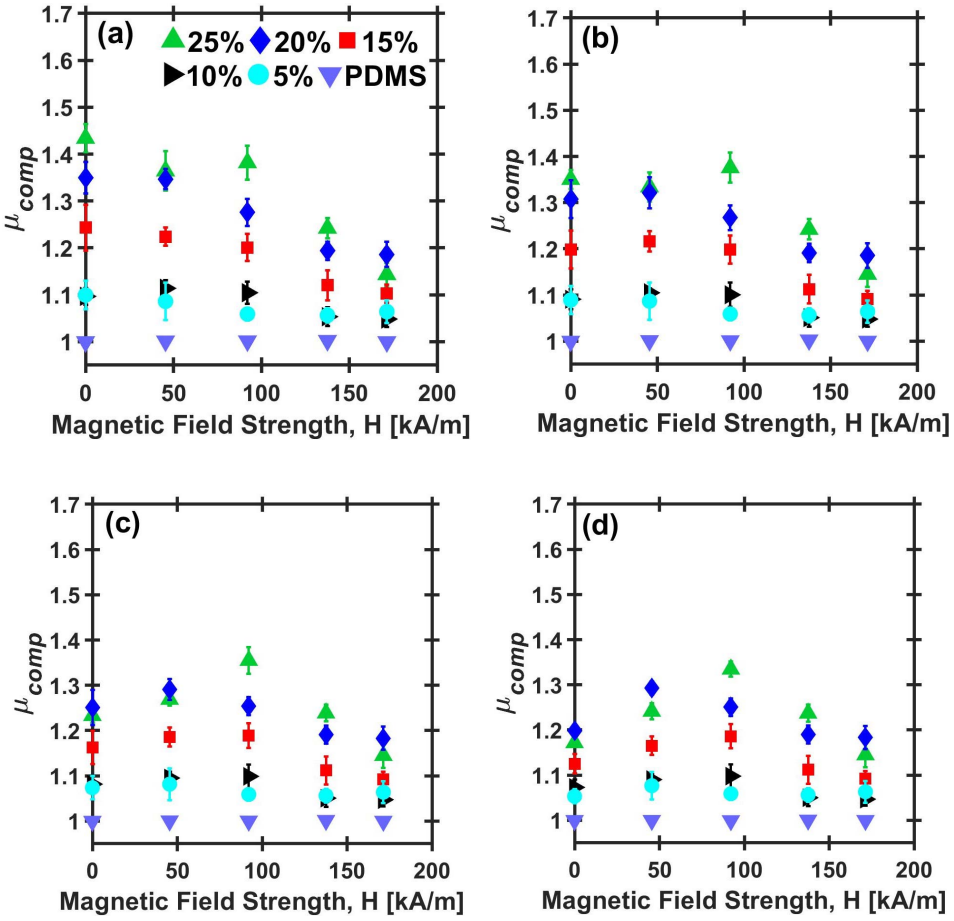

Fig. 5. Variation in the real component of the relative permeability μ_{comp} of a composite with 0% (just PDMS), 5%, 10%, 15%, 20%, and 25% volume loadings of NZF inclusions in PDMS as a function of bias magnetic field strength at (a) 1, (b) 2, (c) 3, and (d) 4 GHz. The values reported are the mean of four measurements with error bars determined using standard deviation.

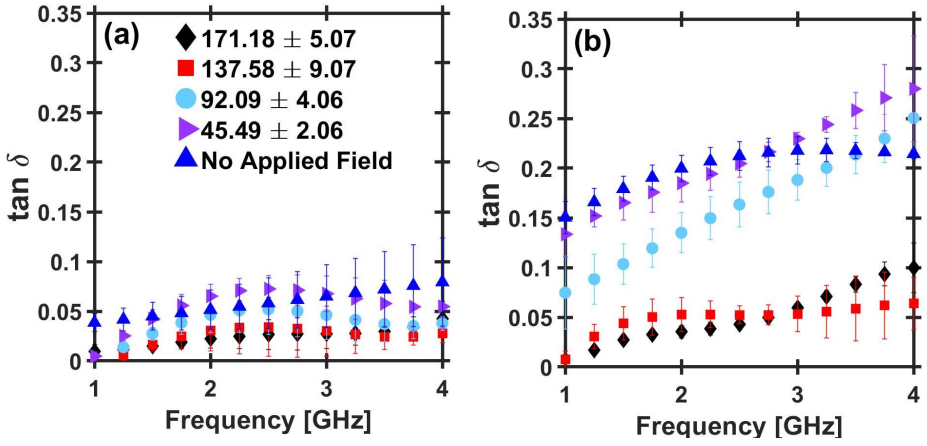

Fig. 6. Magnetic loss tangent tanδ of (a) 5% NZF and (b) 25% NZF composites from 1 to 4 GHz for various external magnetic biasing field. Stronger magnetic biasing fields strongly suppress the magnetic losses for the 25% NZF samples, while increasing the magnetic biasing field has a less noticeable effect on tanδ for the 5% NZF samples. The values reported are the mean of four measurements with error bars determined using standard deviation.

accounting for the intrinsic systematic error associated with the network analyzer and coaxial airline. Samples were then inserted on the center conductor of the coaxial airline and their lengths measured using digital calipers. To mitigate the downtime between measurements, we determined the interior temperature at which the solenoid naturally settled with successive 5, 10, 15, and 20 A measurements under active cooling. With the solenoid at room temperature (21 °C), concurrent measurements at the above currents showed that the interior temperature of the solenoid increased by nearly 9 °C. When allowed to warm to 30 °C, the same current measurements yielded a maximum temperate transient of approximately 3 °C. Thus, we allowed the solenoid's interior to warm to 30 °C to better control and monitor the solenoid's

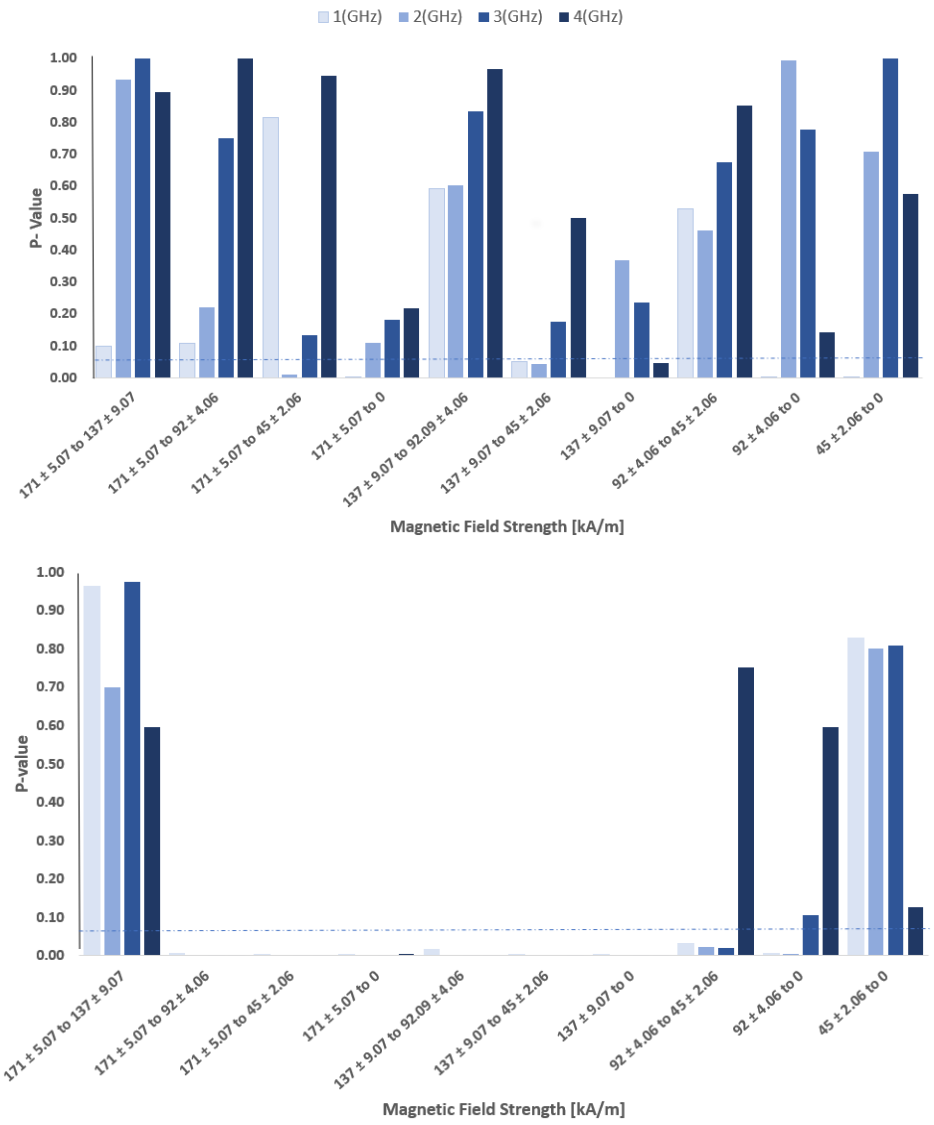

Fig. 7. Results of the ANOVA and multiple comparison test on the magnetic loss tangent tanδ from Fig. 5 for the 5% NZF (top) and 25% NZF (bottom) volume loadings, where $p < 0.05$ indicates statistical significance. High statistical significance was achieved for the 25% NZF magnetic losses which suggests the higher magnetic fields aid in the suppression of the magnetic losses. The statistical significance achieved for 5% NZF was typically achieved at the lowest frequency studied (1 GHz) and when comparing strong to weak magnetic fields (e.g., 171 kA/m to 0).

temperature. Temperature transients inside the coil varied for each measurement since increasing the current increased the heat produced. Fans actively cooled the coil's interior to 30 °C before proceeding to the next measurement.

Using a network analyzer (Keysight FieldFox Handheld Microwave Analyzer N9913A), we measured the S-parameters of the coaxial airline from 1 to 4 GHz at solenoid currents of 0, 5, 10, 15, and 20 A (in that order). The S-parameters were then imported into commercial software (Keysight Material Measurement Suite Software Transmission Line and Free Space method) to calculate the permeability using the Polynomial Fit Reflection/Transmission Mu and Epsilon model, which is an iterative technique to fit material properties to a polynomial that is highly accurate for magnetic samples. The average number of scans per measurement was set to three; the number of points per scan was set to 601; the power was set to −15 dBm; and the intermediate frequency bandwidth (IFBW) was set to 1 kHz. The IFBW and average number of scan parameters are directly related to the overall speed of the measurement. After some trial and error, these settings were chosen to minimize the solenoid's operational time without compromising measurement accuracy.

To determine the statistical significance of the variation in permeability with volume fraction for a given field strength, we wrote a MATLAB script to perform a one-way analysis of variance (ANOVA). The output of the ANOVA test was then used to perform a multiple comparison test utilizing the Tukey–Kramer method to generate a p value that represents the likelihood of the observed value occurring due to chance. The Tukey–Kramer multiple comparison test is optimized for balanced one-way ANOVA tests with equal sample sizes, making it a natural selection for determining statistical significance. The standard used to determine statistical significance

was $\alpha = 0.05$; therefore, $p < 0.05$ indicates statistical significance.

III. Results

A. Single-Inclusion Results

The permeability and magnetic loss tangents of both single- and dual-inclusion composites are strongly coupled to the frequency and bias field strength [14]. The measured real composite permeability μ_{comp} decreased with increasing frequency; however, this behavior only became statistically significant at higher volume loadings of NZF. Figs. 3 and 4 demonstrate this dependence of μ_{comp} for 50% and 25% NZF composites, respectively, at 1, 2, 3, and 4 GHz in the presence of applied magnetic fields of 0, 45.49 $\pm$ 2.06, 92.09 $\pm$ 4.06, 137.58 $\pm$ 9.07, and 171.18 $\pm$ 5.07 kA/m. The 50% NZF composite corresponds to the highest volume loading we could achieve to attempt to approximate the bulk NZF measurements.

The decrease in μ_{comp} with respect to frequency is related to both resonance and relaxation phenomena [28]. The intrinsic relaxation time associated with domain wall rotation, spin magnetic moments, and orbital magnetic moments limits the ability of the material to realign with the field at high frequencies, causing permeability to decrease [28]–[31].

At lower magnetic field strength $H \lesssim 100$ kA/m, μ_{comp} decreased with increasing frequency; for $H \gtrsim 100$ kA/m, μ_{comp} was insensitive to frequency. Also interesting, at 3 and 4 GHz, μ_{comp} increased with increasing H for $H \lesssim 100$ kA/m but decreased with increasing H for $H \gtrsim 100$ kA/m for the 25% NZF samples. Conversely, at 3 and 4 GHz, μ_{comp} only increased for $H \lesssim 50$ kA/m for the 50% NZF composite. This frequency and magnetic field strength dependence of μ_{comp} have implications on NLTL design. NLTLs operating at these frequencies with a sufficiently high-volume fraction of NZF can leverage the observed profile by biasing the composite at the appropriate H. In addition to aiding in coherent precession of the magnetic moments, this also maximizes the difference between μ at the crest of the pulse and the base of the pulse front, maximizing the sharpening of the risetime. Moreover, this capability of manipulating H for controlling phase velocity is promising for incorporating NLTLs into phased array systems to delay pulses using different field strengths [4].

To assess the impact of H on the composite, we considered the statistical significance of the observed changes at each frequency. The ANOVA test revealed that at 1 and 2 GHz, the changes observed for $H \lesssim 100$ kA/m were never statistically significant in the 25% NZF composites; however, $H \gtrsim 100$ kA/m induced statistically significant changes. At 3 and 4 GHz, the only insignificant changes occurred when comparing 45.49 $\pm$ 2.06 to 137.58 $\pm$ 9.07 kA/m and 0 to 171.18 $\pm$ 5.07 kA/m. Given the observed profile at these frequencies, this insignificance intuitively makes sense.

The same statistical analysis was performed on the 50% NZF composite. The changes observed for $H \lesssim 50$ kA/m at 1 and 2 GHz were not statistically significant; however, excluding the 137.58 $\pm$ 9.07 kA/m compared to the 171.18 $\pm$ 5.07 kA/m results, changes observed for $H \gtrsim 50$ kA/m were statistically significant. At 3 and 4 GHz, the changes observed between all field strengths were statistically significant, excluding the comparison between the highest two fields. The insignificance at higher field strengths is to be expected as the composite approaches saturation.

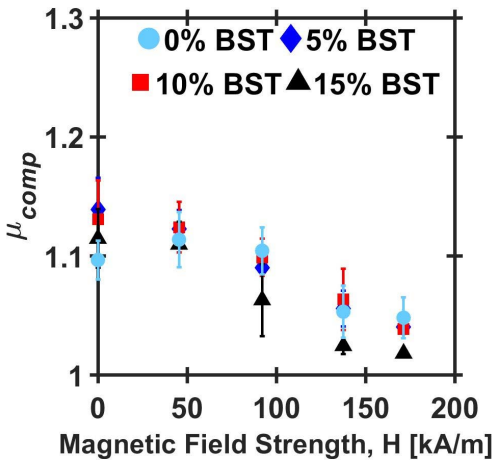

Fig. 8. Relative permeability μ_r of a composite containing 10% NZF and 0%, 5%, 10%, and 15% BST in PDMS as a function of bias magnetic field strength at 1 GHz. The permeability is not affected by the addition of BST. The values reported are the mean of four measurements with error bars determined using standard deviation.

The nonlinear behavior of the permeability with respect to the magnetic field strength is a unique property of ferrimagnetic materials. It occurs because the material undergoes magnetic hysteresis, which describes the relationship between the internal field **B** and applied field **H**. Generally, introducing and gradually increasing the magnetizing field causes the permeability of a ferrous material to briefly increase until reaching a maximum; further increasing the field causes permeability to decrease as it approaches the saturation point [32]. While we observe this behavior for the composites manufactured here, it is not significant until achieving a 15% volume loading, suggesting that some minimum volume fraction is necessary before the influence of the biasing field becomes significant.

Assessing the impact of volume fraction on μ_{comp} is necessary to understand the potential implementation of dielectric and magnetic property manipulation for HPM system flexibility. Fig. 5 shows μ_{comp} as a function of H for various volume fractions of NZF at 1, 2, 3, and 4 GHz. In general, μ_{comp} increases with increasing volume fraction, but this effect is significantly dampened at higher frequencies. Of similar interest is the nonlinearity of the permeability for each respective volume fraction. Significant changes in the permeability with respect to the magnetic field only occur when the NZF volume loadings are $\geq$15%. Fig. 5 also demonstrates the feasibility of using NZF volume loading to tune μ_{comp}, which could suggest the potential to tune NLTL impedance for matching to either a pulsed power driver or an output. Figs. 3–5 also show the ability to control the permeability by using an external biased field to provide the operator greater control over the parameters of the radio frequency (RF) pulse from the NLTL, such as risetime.

The impact of the volume fraction on bulk composites is well-documented for linear materials. In particular, the theory

TABLE II
STATISTICAL SIGNIFICANCE OF THE CHANGES IN μ_{comp} FOR CHANGES IN NZF VOLUME LOADING

Field Strength (kA/m)	f (GHz)	25 to 20	25 to 15	25 to 10	25 to 5	20 to 15	20 to 10	20 to 5	15 to 10	15 to 5	10 to 5
0		0.05	**< 0.01**	**< 0.01**	**< 0.01**	**0.01**	**< 0.01**	**< 0.01**	**< 0.01**	**< 0.01**	1.00
45 ± 2.06		0.95	**< 0.01**	**< 0.01**	**< 0.01**	**< 0.01**	**< 0.01**	**< 0.01**	**< 0.01**	**< 0.01**	0.78
92 ± 4.06	1	**< 0.01**	**< 0.01**	**< 0.01**	**< 0.01**	**0.03**	**< 0.01**	**< 0.01**	**< 0.01**	**< 0.01**	0.29
137 ± 9.07		0.14	**< 0.01**	**< 0.01**	**< 0.01**	0.09	**< 0.01**	**< 0.01**	**0.04**	0.05	1.00
171 ± 5.07		0.12	0.77	**< 0.01**	**0.01**	**0.01**	**< 0.01**	**< 0.01**	**0.02**	0.08	0.93
0		0.51	**< 0.01**	**< 0.01**	**< 0.01**	**0.01**	**< 0.01**	**< 0.01**	**0.01**	**0.01**	1.00
45 ± 2.06		0.98	**< 0.01**	**< 0.01**	**< 0.01**	**< 0.01**	**< 0.01**	**< 0.01**	**< 0.01**	**< 0.01**	0.94
92 ± 4.06	2	**< 0.01**	**< 0.01**	**< 0.01**	**< 0.01**	**0.04**	**< 0.01**	**< 0.01**	**< 0.01**	**< 0.01**	0.36
137 ± 9.07		0.12	**< 0.01**	**< 0.01**	**< 0.01**	**0.04**	**< 0.01**	**< 0.01**	0.07	0.11	1.00
171 ± 5.07		0.20	0.50	**< 0.01**	**0.01**	**0.01**	**< 0.01**	**< 0.01**	**0.04**	0.16	0.92
0		0.93	0.06	**< 0.01**	**< 0.01**	**0.01**	**< 0.01**	**< 0.01**	**0.02**	**0.01**	1.00
45 ± 2.06		0.98	**0.02**	**< 0.01**	**< 0.01**	**0.01**	**< 0.01**	**< 0.01**	**0.01**	**< 0.01**	0.97
92 ± 4.06	3	**< 0.01**	**< 0.01**	**< 0.01**	**< 0.01**	**0.03**	**< 0.01**	**< 0.01**	**< 0.01**	**< 0.01**	0.30
137 ± 9.07		0.12	**< 0.01**	**< 0.01**	**< 0.01**	0.05	**< 0.01**	**< 0.01**	0.06	0.09	1.00
171 ± 5.07		0.19	0.48	**< 0.01**	**0.01**	**0.01**	**< 0.01**	**< 0.01**	**0.03**	0.16	0.91
0		0.28	**0.02**	**< 0.01**	**< 0.01**	**< 0.01**	**< 0.01**	**< 0.01**	**0.01**	**< 0.01**	0.54
45 ± 2.06		0.77	**0.03**	**< 0.01**	**< 0.01**	**< 0.01**	**< 0.01**	**< 0.01**	**0.03**	**0.01**	0.97
92 ± 4.06	4	**< 0.01**	**< 0.01**	**< 0.01**	**< 0.01**	**0.02**	**< 0.01**	**< 0.01**	**< 0.01**	**< 0.01**	0.22
137 ± 9.07		0.14	**< 0.01**	**< 0.01**	**< 0.01**	**0.04**	**< 0.01**	**< 0.01**	0.05	0.09	1.00
171 ± 5.07		0.20	0.48	**< 0.01**	**0.01**	**0.01**	**< 0.01**	**< 0.01**	**0.03**	0.15	0.92

Values in **bold** indicate statistical significance ($p < 0.05$)

has been well established through the development of effective medium theories (EMTs), which can predict composite material properties, such as permeability, permittivity, and conductivity [33], [34]. The increase in permeability with increasing volume fraction is well predicted by EMTs, but the accuracy of these theories is typically limited to lower volume fractions. Experimentally, this behavior has been observed in numerous studies, although Fiske *et al*. [26], [27] more directly appeal to this behavior with respect to ferrite volume loading.

Table II summarizes the results of ANOVA to assess the statistical significance of the differences and changes induced in μ_{comp} by altering the volume fraction. At all frequencies, the data for 10% NZF compared to the 5% NZF were never statistically significant. The difference between 25% NZF and 20% NZF was only significant at $H = 92.09 \pm 4.06$ kA/m. Changing the volume fraction by more than 10% caused statistically significant differences in μ_{comp} for most field strengths and volume loading changes. The reduced statistical significance at higher field strengths is expected as we approach the saturation permeability. These results suggest that inclusion loading should be modified by at least 10% to induce noticeable changes in μ_{comp}.

It is also critical to consider a material's magnetic losses when considering implementation into an NLTL system, specifically the dependence of the magnetic loss tangent on frequency and bias field strength. Fig. 6 shows the magnetic loss tangent tanδ, given by the ratio of the imaginary permeability to the real permeability, for composites comprising either 5% NZF or 25% NZF from 1 to 4 GHz as a function of H. As expected, the magnetic losses are heavily influenced by the volume fraction of NZF and frequency. Interestingly, the magnetic losses of the 25% NZF composite are strongly coupled to the external field strength, indicating the importance of adding more nonlinear inclusions into the composite. The results suggest that applying stronger external magnetic field strengths of 137.58 ± 9.07 and 171 ± 5.07 kA/m may suppress magnetic losses compared to no/low magnetic field strength. Equally important is that the magnetic loss tangents tend to be fairly small, which is necessary to achieve microwave oscillations [4].

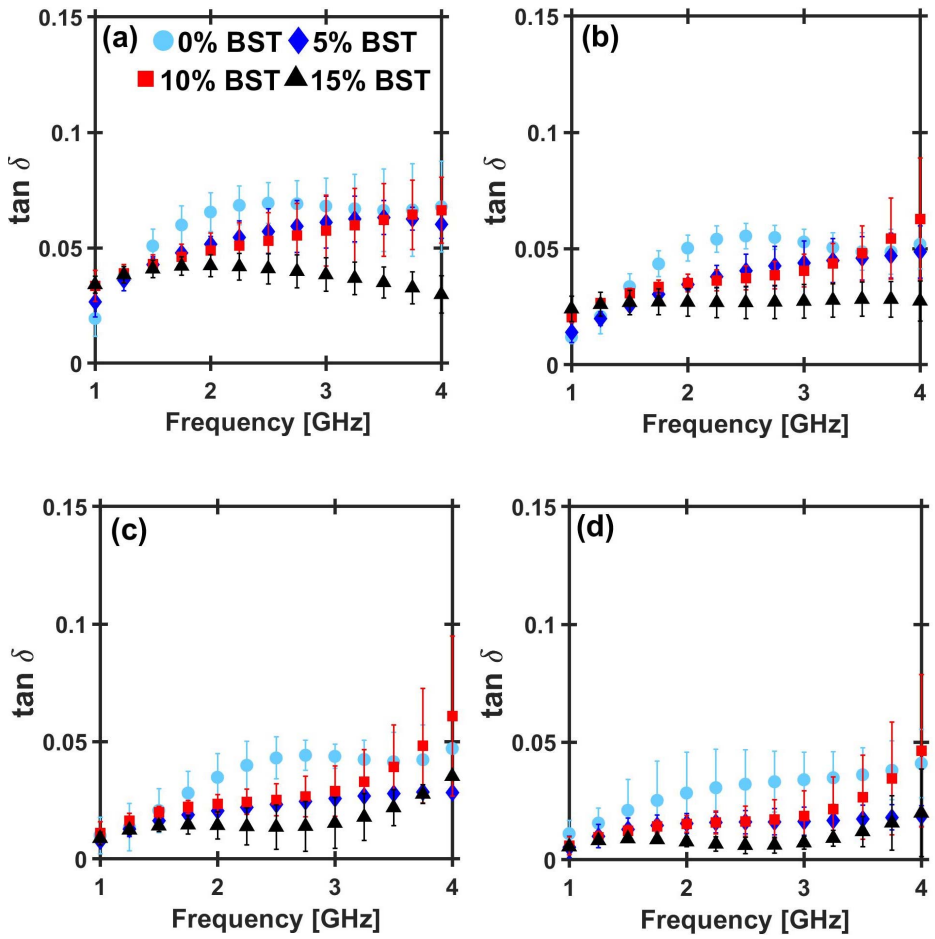

Fig. 9. Magnetic losses for a 10% NZF composite with varying volume fractions of BST at (a) 45 ± 2.06, (b) 92 ± 4.06, (c) 137 ± 9.07, and (d) 171 ± 5.07 kA/m from 1 to 4 GHz.

Fig. 7 presents the results of the ANOVA test performed to assess the statistical significance of the data in Fig. 5. For 5% NZF, changes in the magnetic bias were generally only statistically significant at the lowest frequency when comparing the higher applied magnetic bias to no bias (e.g., 171 kA/m compared to 0 kA/m at 1 GHz). The changes observed for the 25% NZF data exhibit statistical significance across the entire frequency range for most magnetic field biases. This suggests that H plays a role in suppressing the magnetic losses at 25% NZF. Therefore, when designing a composite-based NLTL system utilizing ferrimagnetic material, external magnetic fields at higher volume loadings may minimize (or at least mitigate) the magnetic losses, which is advantageous for maximizing the efficiency of the system. These results also demonstrate the importance of using a pulse of sufficient current to maximize the magnetic field inside the NLTL to reduce the magnetic losses.

B. Dual-Inclusion Results

Dual-inclusion composites containing various volume fractions of BST and NZF were manufactured and subjected to the same test methods as the single inclusion. Fig. 8 shows that adding BST inclusions to a composite containing 10% NZF in PDMS will not influence μ_{comp}. This is advantageous because, while not measured here, adding BST inclusions increase the composite's permittivity, which should theoretically reduce the risk of breakdown between the center and outer conductors while still permitting the use of H for biasing the NZF. Moreover, since BST exhibits nonlinear permittivity with electric field, combining BST and NZF may permit simultaneously achieving nonlinearity in both permittivity and permeability to form an electromagnetic shock wave.

The ANOVA test performed on the data from Fig. 8 and summarized in Table III confirms that adding BST to a composite with NZF generally does not change μ_{comp} significantly. It required the highest BST volume loading (15%) and highest magnetic field strength (171 kA/m) considered here to cause a statistically significant change in μ_{comp} compared to the 10% NZF sample.

Fig. 9 shows the effect of BST volume loading on magnetic loss tangent for a 10% NZF composite. In general, the changes observed were not statistically significant for much of the frequency range; however, the difference between the 10% NZF/15% BST loading and the 10% NZF composite was statistically significant. This is surprising since BST is inherently nonmagnetic and warrants further investigation into characterizing the potential mechanisms by which BST may suppress magnetic losses. A similar effect was seen in [1]. One potential reason could be that adding a sufficient volume

TABLE III
STATISTICAL SIGNIFICANCE OF ADDING BST ON μ_{comp} OF A 10% NZF SAMPLE

Field Strength (kA/m)	171 ± 5.07	137 ± 9.07	92 ± 4.06	45 ± 2.06
5% to 10%	1.00	0.95	0.97	1.00
5% to 15%	0.05	0.21	0.53	0.82
5% to 0%	0.70	1.00	0.89	0.93
10% to 15%	0.06	0.09	0.31	0.78
10% to 0%	0.58	0.90	0.99	0.90
15% to 0%	**0.01**	0.27	0.21	0.99

TABLE IV
STATISTICAL SIGNIFICANCE OF ADDING BST ON THE MAGNETIC LOSS TANGENT OF A 10% NZF COMPOSITE

Frequency (GHz)	Field Strength (kA/m)	5% to 0%	10% to 0%	15% to 0%
1	45 ± 2.06	0.527	0.056	**0.044**
	92 ± 4.06	0.814	**0.013**	**0.010**
	137 ± 9.07	0.940	0.991	0.991
	171 ± 5.07	0.360	0.391	0.389
2	45 ± 2.06	0.076	**0.021**	**<0.01**
	92 ± 4.06	**<0.01**	**<0.01**	**<0.01**
	137 ± 9.07	0.064	0.121	**<0.01**
	171 ± 5.07	0.389	0.315	0.095
3	45 ± 2.06	0.875	0.626	**0.030**
	92 ± 4.06	0.416	0.156	**<0.01**
	137 ± 9.07	**0.048**	0.077	**<0.01**
	171 ± 5.07	0.118	0.146	**0.015**
4	45 ± 2.06	0.867	0.998	**<0.01**
	92 ± 4.06	0.995	0.838	0.303
	137 ± 9.07	0.603	0.762	0.854
	171 ± 5.07	0.539	0.984	0.585

In general, adding 5% or 10% BST to NZF does not result in a statistically significant change in loss tangent ($p > 0.05$).

loading of BST, which is strongly insulative, disrupts the connectivity of the NZF inclusions, subsequently reducing the strength of the magnetic behavior or losses to eddy currents. Further supporting this argument is the size of the BST particles (∼600–800 nm), which allows it to wedge between the much larger NZF. Table IV reports the p values from the ANOVA (∼600–800 nm).

IV. CONCLUSION

This article reports the nonlinear permeability of composites containing various volume loadings of NZF or combinations of NZF and BST between 1 and 4 GHz. The permeability of the NZF composites strongly depended on frequency, external magnetic field strength, and volume loading. Statistically significant changes in the composite's permeability with respect to the magnetic field strength required NZF volume loadings of at least 15% NZF. Statistically significant changes in the permeability with respect to volume loading required at least a 10% change in NZF volume loading at most magnetic field strengths, although composites with 5% changes in NZF volume loading were, on average, statistically significant at low magnetic field strengths but became insignificant at higher magnetic field strengths. When investigating the effect of frequency on the composites, the observed profile suggested that NLTLs at 3 and 4 GHz could leverage biasing the line at the appropriate H to maximize the line pulse sharpening and microwave generation capabilities. This phenomenon would occur since the permeability seen by the crest of the pulse and foot of the pulse would be maximized. For dual-inclusion composites, adding BST did not induce statistically significant changes in the permeability except when comparing a 15% BST/10% NZF to a 0% BST/10% NZF sample at 171 kA/m. The magnetic loss tangents for single- and dual-inclusion composites strongly depended on the magnetic field strength, generally exhibiting lower loss tangents at higher external field values. For dual-inclusion composites, adding a sufficient volume loading of BST to the NZF composite suppressed magnetic losses. Future studies may explore whether this behavior arises due to the total volume loading of all (NZF and BST) inclusions or BST disrupting the NZF network, reducing the magnetic effects.

Long-term, characterizing the behavior of these composites will permit the construction of composite-based NLTLs with various nonlinear permittivity and permeability. This flexibility may permit tuning the output RF from the NLTL or matching the NLTL to a given load based on adjusting the volume loading of nonlinear dielectric or magnetic inclusions. Of particular importance, changing the composition of NZF can change its permeability, which can then alter the composite permeability. The approach and results presented here provide a process for measuring and assessing the nonlinear permeability for such materials.

ACKNOWLEDGMENT

This work was supported by the Office of Naval Research under Grant N00014-18-1-2341.

REFERENCES

[1] K. M. Noel, A. M. Pearson, R. D. Curry, and K. A. O'Connor, "High frequency properties of high voltage barium titanate-ferrite multiferroic metamaterial composites," *IEEE Trans. Dielectr. Electr. Insul.*, vol. 23, no. 5, pp. 2965–2969, Oct. 2016.

[2] J. Gaudet, E. Schamiloglu, J. O. Rossi, C. J. Buchenauer, and C. Frost, "Nonlinear transmission lines for high power microwave applications—A survey," in *Proc. IEEE Int. Power Modulators High-Voltage Conf.*, May 2008, pp. 131–138.

[3] A. J. Fairbanks, A. M. Darr, and A. L. Garner, "A review of nonlinear transmission line system design," *IEEE Access*, vol. 8, pp. 148606–148621, 2020.

[4] J.-W.-B. Bragg, J. C. Dickens, and A. A. Neuber, "Ferrimagnetic nonlinear transmission lines as high-power microwave sources," *IEEE Trans. Plasma Sci.*, vol. 41, no. 1, pp. 232–237, Jan. 2013.

[5] J.-W.-B. Bragg, J. C. Dickens, and A. A. Neuber, "Material selection considerations for coaxial, ferrimagnetic-based nonlinear transmission lines," *J. Appl. Phys.*, vol. 113, no. 6, Feb. 2013, Art. no. 064904.

[6] D. V. Berkov and J. Miltat, "Spin-torque driven magnetization dynamics: Micromagnetic modeling," *J. Magn. Magn. Mater.*, vol. 320, no. 7, pp. 1238–1259, Apr. 2008.

[7] E. G. L. Rangel, J. O. Rossi, J. J. Barroso, F. S. Yamasaki, and E. Schamiloglu, "Practical constraints on nonlinear transmission lines for RF generation," *IEEE Trans. Plasma Sci.*, vol. 47, no. 1, pp. 1000–1016, Jan. 2019.

[8] G. Branch and P. W. Smith, "Shock waves in transmission lines with nonlinear dielectrics," in *Proc. IEE Colloq. Pulsed Power*, Feb. 1993, pp. 7-1–7-3.

[9] A. L. Garner, G. J. Parker, and D. L. Simone, "A semi-empirical approach for predicting the performance of multiphase composites at microwave frequencies," *IEEE Trans. Dielectr. Electr. Insul.*, vol. 23, no. 2, pp. 1126–1134, Apr. 2016.

[10] A. L. Garner, G. J. Parker, and D. L. Simone, "Predicting effective permittivity of composites containing conductive inclusions at microwave frequencies," *AIP Adv.*, vol. 2, no. 3, Sep. 2012, Art. no. 032109.

[11] A. L. Garner, G. J. Parker, and D. L. Simone, "Accounting for conducting inclusion permeability in the microwave regime in a modified generalized effective medium theory," *IEEE Trans. Dielectr. Electr. Insul.*, vol. 22, no. 4, pp. 2064–2072, Aug. 2015.

[12] Z. Wang *et al.*, "Effect of high aspect ratio filler on dielectric properties of polymer composites: A study on barium titanate fibers and graphene platelets," *IEEE Trans. Dielectr. Electr. Insul.*, vol. 19, no. 3, pp. 960–967, Jun. 2012.

[13] J. T. Allanson, "The permeability of ferromagnetic materials at frequencies between 10^5 and 10^{10} c/s," *J. Inst. Electr. Eng. III Radio Commun. Eng.*, vol. 92, no. 20, pp. 247–255, 1945.

[14] M. Zhang *et al.*, "Size effects on magnetic properties of $Ni_{0.5}Zn_{0.5}Fe_2O_4$ prepared by sol-gel method," *Adv. Mater. Sci. Eng.*, vol. 2013, Jul. 2013, Art. no. 609819.

[15] X. Wen, S. J. Kelly, J. S. Andrew, and D. P. Arnold, "Nickel-zinc ferrite/permalloy ($Ni_{0.5}Zn_{0.5}Fe_2O_4$/Ni-Fe) soft magnetic nanocomposites fabricated by electro-infiltration," *AIP Adv.*, vol. 6, no. 5, May 2016, Art. no. 056111.

[16] A. Verma, A. K. Saxena, and D. C. Dube, "Microwave permittivity and permeability of ferrite–polymer thick films," *J. Magn. Magn. Mater.*, vol. 263, nos. 1–2, pp. 228–234, Jul. 2003.

[17] L. Yan, J. Wang, Y. Ye, Z. Hao, Q. Liu, and F. Li, "Broadband and thin microwave absorber of nickel–zinc ferrite/carbonyl iron composite," *J. Alloys Compounds*, vol. 487, nos. 1–2, pp. 708–711, Nov. 2009.

[18] A. Ahmad, Z. Abbas, S. Obaiys, and D. Abdalhadi, "Improvement of dielectric, magnetic and thermal properties of OPEFB fibre–polycaprolactone composite by adding Ni–Zn ferrite," *Polymers*, vol. 9, no. 12, Feb. 2017, Art. no. 12.

[19] A. M. A. Henaish, M. Mostafa, B. I. Salem, and O. M. Hemeda, "Improvement of magnetic and dielectric properties of magnetoelectric BST-NCZMF nano-composite," *Phase Transitions*, vol. 93, no. 5, pp. 470–490, May 2020.

[20] K. N. Rozanov, Z. W. Li, L. F. Chen, and M. Y. Koledintseva, "Microwave permeability of Co_2Z composites," *J. Appl. Phys.*, vol. 97, no. 1, Jan. 2005, Art. no. 013905.

[21] P. Singh, V. K. Babbar, A. Razdan, R. K. Puri, and T. C. Goel, "Complex permittivity, permeability, and X-band microwave absorption of CaCoTi ferrite composites," *J. Appl. Phys.*, vol. 87, no. 9, pp. 4362–4366, May 2000.

[22] J. S. Ghodake, R. C. Kambale, T. J. Shinde, P. K. Maskar, and S. S. Suryavanshi, "Magnetic and microwave absorbing properties of Co^{2+} substituted nickel–zinc ferrites with the emphasis on initial permeability studies," *J. Magn. Magn. Mater.*, vol. 401, pp. 938–942, Mar. 2016.

[23] M. D. Rintoul and S. Torquato, "Precise determination of the critical threshold and exponents in a three-dimensional continuum percolation model," *J. Phys. A, Math. Gen.*, vol. 30, no. 16, pp. L585–L592, Aug. 1997.

[24] V. K. S. Shante and S. Kirkpatrick, "An introduction to percolation theory," *Adv. Phys.*, vol. 20, no. 85, pp. 325–357, 1971.

[25] D. M. Grannan, J. C. Garland, and D. B. Tanner, "Critical behavior of the dielectric constant of a random composite near the percolation threshold," *Phys. Rev. Lett.*, vol. 46, no. 5, pp. 375–378, Feb. 1981.

[26] T. J. Fiske, H. S. Gokturk, and D. M. Kalyon, "Percolation in magnetic composites," *J. Mater. Sci.*, vol. 32, no. 20, pp. 5551–5560, 1997.

[27] T. J. Fiske, H. Gokturk, and D. M. Kalyon, "Enhancement of the relative magnetic permeability of polymeric composites with hybrid particulate fillers," *J. Appl. Polym. Sci.*, vol. 65, no. 7, pp. 1371–1377, Aug. 1997.

[28] D. Stillman and G. Olhoeft, "Frequency and temperature dependence in electromagnetic properties of Martian analog minerals," *J. Geophys. Res.*, vol. 113, no. E9, 2008, Art. no. E09005.

[29] T. Tsutaoka, "Frequency dispersion of complex permeability in Mn–Zn and Ni–Zn spinel ferrites and their composite materials," *J. Appl. Phys.*, vol. 93, no. 5, pp. 2789–2796, Mar. 2003.

[30] N. Bowler, "Frequency-dependence of relative permeability in steel," *AIP Conf. Proc.*, vol. 82, pp. 1269–1276, Mar. 2006.

[31] G. Rado, R. Wright, and W. Emerson, "Ferromagnetism at very high frequencies," *Phys. Rev. Lett.*, vol. 80, no. 1947, pp. 273–281, 1950.

[32] J. Tang, W. Liu, Y. He, and X. Xue, "Effect of biasing magnetic field on the complex permeability of nanocrystalline $Fe_{86}Zr_7B_6Cu_1$ alloy," *Phys. B, Condens. Matter*, vol. 389, no. 2, pp. 343–346, Feb. 2007.

[33] X. Zhu, "Assessing effective medium theories for designing composites for nonlinear transmission lines," M.S. thesis, School Nucl. Eng., Purdue Univ., West Lafayette, IN, USA, 2019.

[34] A. H. Sihvola, *Electromagnetic Mixing Formulas and Applications*. London, U.K.: IET, 1999.